Chemistry and Materials

The Center for Science Innovation

Research Article

Chem. Mater. Vol. (No.) 2026, page

Transmetallation Reaction of Alkali and Alkaline-earth Metal Ions in Supramolecular Complex of $[\{Au_6Cd_3(tdme)_2(D\text{-}pen)_6\}Cd_4Na_4](NO_3)_{12}$

Benny Wahyudianto[1,*], Tatsuhiro Kojima[1,2], Nobuto Yoshinari[1], Takumi Konno[1,3,*]

[1]Department of Chemistry, Graduate School of Science, The University of Osaka, 1-1 Machikaneyamacho, Toyonaka, Osaka 560-0043, Japan

[2]Department of Applied Chemistry, Kobe City College of Technology, Kobe 651-2194, Japan

[3]Department of Chemistry, College of Science, National Taiwan Normal University, Taipei 11677, Taiwan

*Corresponding authors: benny.wahyudianto@aist.go.jp; konno@ntnu.edu.tw

Received
06 January 2026

Received in revised form
16 February 2026

Accepted
01 March 2026

Published online
06 April 2026

DOI
xxx

Abstract

One of the advantages of coordination complex with a framework structure is that it facilitates conducting metal exchange reaction or transmetallation, which important for several purposes. In this study, we evaluated transmetallation phenomena in a 116 nuclear complex of $[\{Au_6Cd_3(tdme)_2(D\text{-}pen)_6\}_{12}Cd_4Na_4](NO_3)_{12}$ (**1**$_{CdNa}$) using monovalent and divalent metal ions from alkali and alkaline-earth groups, respectively. The metal replacements were carried out in high concentration solution through single-crystal-to-single-crystal manner. The observation focused on the structural refinement based on single-crystal X-ray diffraction data. The results indicated that selective metal exchange occurred exclusively in specific locations. The presence of *d*-orbital and metal coordination preferences became two pivotal factors to proceed transmetallation in **1**$_{CdNa}$.

Keywords: metal exchange reaction, single-crystal-to-single-crystal, X-ray crystallography

1. Introduction

Recently, the utilization of host material has grown exponentially since they can address various challenges, such as adsorption/desorption, separation of chiral or non-chiral molecules, catalyst support, trapping agent, etc. [1-6]. The materials span from natural to synthetic products, where each offers distinct benefits and limitations [5-8]. Host materials are often discussed together with porous materials, whose pore size (micro-, meso-, or nanoporous) are typically characterized using BET isotherm analysis [9]. Previously, such benefits were obtained using silica-based materials such as zeolites, which were chemically modified by using acidic or basic treatments [10]. In parallel, the development of porous materials has advanced significantly, especially bottom-up approach with self-assembly synthesis method. The structure arrangement employed covalent coordination bond between metal center and organic ligands (i.e., organic molecules or metalloligand) [11-12]. At the molecular level, the dimensionality and continuity of these porous materials could be predicted practically, enabling researchers to perform rational molecular architecture [13-16]. To date, the investigations into the effect of diverse metal centers and organic ligands continue to process, yielding promising outcomes across numerous applications [17-18].

The strength of interaction between a metal centers and its coordinating ligands depends on the type of metal ion and the environment surrounding the ligand's functional group. One way to evaluate the interaction is through metal exchange process, commonly referred to as transmetallation [11,19]. In single crystal, transmetallation could be facilitated via a single-crystal-to-single-crystal (SCSC) manner, in which the crystal can keep its crystallinity before and after metal replacement process

[20]. This transformation was also suitable to characterize by using single-crystal X-ray diffraction (SCXRD).

Our group has synthesized several coordination complexes that function as frameworks, which are capable to undergo transmetallation reactions. For example, 116-nuclear supramolecular complex composed of $[\{Au_6Cd_3(tdme)_2(D\text{-}pen)_6\}_{12}Cd_4Na_4](NO_3)_{12}$ (**1**$_{CdNa}$) (tdme=1,1,1-tris(diphenylphosphinomethyl)ethane, D-pen^{2-} = D-penicillaminate). Using **1**$_{CdNa}$, we achieved one of the fastest transmetallation reactions among coordination complexes and metal organic frameworks [**11**]. Also, we observed a stepwise transmetallation process from Cd^{II}/Na^{I} to Co^{II}, as well as partial metal exchange replacement with Zn^{II} and Mn^{II}, and linker substitution with Cd^{II} [11,19].

In this investigation, we sought to expand the scope of metal ion variability by employing alkali (e.g., Li^{I}, K^{I}, Rb^{I}, or Cs^{I}) and alkaline-earth metal ions (e.g., Ca^{II} or Sr^{II}) to evaluate the stability of Cd^{II} metal center and Cd^{II}/Na^{I} linker atoms. The analysis focused on structural change observation through SCXRD, complemented by spectroscopic evidence to support the proposed structural transformations.

2. Materials and Method

2.1. Materials

All chemicals were used without further purification: $LiNO_3$ (Sigma Aldrich), KNO_3, $RbNO_3$, $CsNO_3$, $Ba(NO_3)_2$ (Fujifilm Wako Pure Medicine Co., Ltd.), $Sr(NO_3)_2$ (Merck). The **1**$_{CdNa}$ synthesis pathway was prepared under the same conditions as in references [11].

2.2. Physical measurement

X-ray fluorescence analyses were performed on a SHIMADZU EDX-900 spectrometer. Elemental analyses (C, H, N) were performed at Osaka University using Yanaco CHN Corder MT-5. ^{23}Na and ^{131}Cs NMR analysis were recorded with a JEOL ECAMX-400SP spectrometer in D_2O.

2.3. Single-crystal X-ray diffraction determination

The single-crystal synchrotron-radiation X-ray diffraction measurement of **2**, **3**, **4**, and **5** were carried out on a PILATUS3 X CdTe 1 m area detector (Dectris, Baden, Switzerland) with synchrotron radiation at the BL02B1 beamline in SPring-8 at −173°C. The intensity data were collected by the ω-scan technique, and the diffraction images were processed using RAPID-AUTO. After all the solvated water molecules were removed from the model, the crystal data of was treated by SQUEEZE in the PLATON package. The structures of all crystals were solved by direct methods using SHELXS2015. The structure refinements of all crystals were carried out using full matrix least-squares (SHELXL2015). Many constraints and restraints were required to obtain chemically reasonable molecular structures.

CCDC 2530778, 2530983, 2530984, and 2530985 (**2**, **3**, **4**, and **5**, respectively), contain the supplementary crystallographic data for this paper. These data are provided free of charge by The Cambridge Crystallographic Data Centre (https://www.ccdc.cam.ac.uk/).

2.3. SCSC reaction of 1$_{CdNa}$ with monovalent and divalent metal ions for transmetallation

The single crystals of **1**$_{CdNa}$ were immersed into 1 M of reaction solution containing $LiNO_3$ and kept at room temperature for three days. After immersion, the treated crystals were analyzed by SCXRD and related spectroscopies. The same treatment was applied using other metal ion-containing solutions, such as KNO_3, $RbNO_3$, $CsNO_3$, $Ba(NO_3)_2$, and $Sr(NO_3)_2$ to evaluate the corresponding metal-exchange behavior.

3. Results and Discussion

3.1. Single-crystal X-ray analysis of complex 2, 3, 4, and 5.

Since **1**$_{CdNa}$ possessed a three-dimensional porous structure, it allows facile access for metal-ion replacement, such as that observed for Mn^{II}, Co^{II}, Cu^{II}, Zn^{II}, and Cd^{II} [11,19]. Building on this property, we extended the investigation to include alkali and alkaline-earth metal ions in order to transmetallation behavior in **1**$_{CdNa}$ complex. The transmetallation was conducted through SCSC manned in metal-ion solution at high concentration. For example, Li^{I}, K^{I}, Rb^{I}, Cs^{I}, Ba^{II}, and Sr^{II}. In the case of crystal appearance, immersion of **1**$_{CdNa}$ single crystals in several metal-ion solutions yielded colorless cubic single crystals after 3 days. Their appearance remained almost identical to the original **1**$_{CdNa}$. Here, all obtained single crystals were suitable for SCXRD measurements.

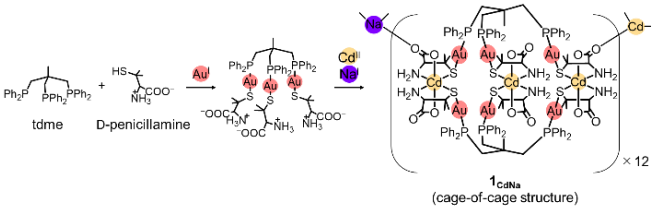

Scheme 1. The synthesis pathway of **1**$_{CdNa}$.

Single crystal X-ray analysis confirmed that all crystals exhibited sufficient diffraction quality for the structural refinement. However, a similar **1**$_{CdNa}$ framework could not be resolved following by the immersion treatment in Rb^{I} or Ba^{II} solutions. In contrast, the immersion of **1**$_{CdNa}$ complex in Li^{I} (**2**), K^{I} (**3**), Cs^{I} (**4**), and Sr^{II} (**5**), adopted Cubic crystal system with the *F*432 space group (Table 1). The lattice parameter and crystal volume of **2**, **3**, and **4** were

comparable to the original **1**$_{CdNa}$ (a = 77.3910 - 78.1019 Å and V = 463,523 - 476,414 Å^3), although **5** showed a slightly increased if it compared to the parent crystal. In an asymmetric unit of **1**$_{CdNa}$, each Cd^{II} metal centers bound to two penicillamine via *cis*-N_2, *trans*-O_2, and *cis*-S_2 in geometry. Three Cd^{II} centers connected through six Au^{I} ions and two tdme ligands forming "cage-type structure". Furthermore, four Cd^{II} and four Na^{I} linker atoms promoted the assembly of a larger supramolecular architecture containing 12 cage structures and a total of 116 nuclearity described as "cage-of-cage structure" (Scheme 1, see Ref. 11). In the transmetallation, the SCXRD observation focused on three Cd^{II} centers and Cd^{II}/Na^{I} linker atoms in the asymmetric unit (Fig. 1).

Table 1. Crystallographic data of **1**$_{CdNa}$, **2**, **3**, **4**, and **5.**

Complex	**1**$_{CdNa}$[11]	**2**	**3**	**4**	**5**
CCDC No.	1909823	2530778	2530983	2530984	2530985
Color, form	Colorless, cubic	Colorless, cubic	Colorless, cubic	Colorless, cubic	Colorless, cubic
λ=Wavelength/ Å	0.600	0.4148	0.4148	0.4148	0.4148
Crystal system	Cubic	Cubic	Cubic	Cubic	Cubic
Space group	*F*432	*F*432	*F*432	*F*432	*F*432
a/Å	76.702(1)	77.5868(19)	77.7363(14)	78.1019(14)	77.2932(14)
b/Å	76.702(1)	77.5868(19)	77.7363(14)	78.1019(14)	77.2932(14)
c/Å	76.702(1)	77.5868(19)	77.7363(14)	78.1019(14)	77.2932(14)
α/°	90	90	90	90	90
β/°	90	90	90	90	90
γ/°	90	90	90	90	90
V/Å^3	451246(4)	467050(34)	469,755(25)	476,414(26)	461,768(25)
T/K	100(2)	100	293	100.15	293
F(000)	173504	250344	194880	327120	298224
ρ_{calcd}/g·cm^{-3}	1.335	2.054	1.447	2.66	2.475
$\mu(\lambda)$/mm^{-1}	4.095	4.794	1.775	5.402	5.553
Flack parameter	0.1165(18)	0.029(4)	0.010(3)	0.041(3)	0.060(3)
Limiting indices	-116 ≤ h ≤ 116 -116 ≤ k ≤ 116 -116 ≤ l ≤ 116	-96 ≤ h ≤ 100 -100 ≤ k ≤ 100 -100 ≤ l ≤ 100	-91 ≤ h ≤ 93 -93 ≤ k ≤ 93 -81 ≤ l ≤ 93	-101 ≤ h ≤ 101 -101 ≤ k ≤ 100 -99 ≤ l ≤ 101	-95 ≤ h ≤ 100 -90 ≤ k ≤ 100 -100 ≤ l ≤ 100
$R1$ (I>2σ(I))[a]	0.0758	0.0573	0.0431	0.0583	0.0446
w$R2$ (all data)[b]	0.2325	0.1752	0.1232	0.1776	0.1328
GOF	1.055	0.963	1.080	1.016	1.022

[a] $R1 = \Sigma||F_o|-|F_c|| / \Sigma|F_o|$.
[b] $wR2 = [\Sigma(w(F_o^2-F_c^2)^2) / \Sigma w(F_o^2)^2]^{1/2}$.

In **2**, structure refinement indicated that the presence of Cd^{II} ion at metal-center and linker positions. However, the position of Na^{I} linker atom in **2** could be distinguished (Fig. 1). A quantitative ^{6}Li-NMR showed a signal at δ = -2.82 ppm, consistent with substitution of Na^{I} by Li^{I} at linker site although the exact position could not be determined due to a weak electron density of Li. In **3**, the crystal structure was closely resembled that of **2**, showing a linker replacement from Na^{I} to K^{I}. An easy penetration of Li^{I} or K^{I} to kick out Na^{I} supported our statement that Na^{I} provided weak interaction in **1**$_{CdNa}$, wherein the position could be replaced by Co^{II} within less than an hour (see Ref. 19). The present of K in **3** was clearly confirmed by SCXRD and XRF analysis (Fig. 1). In the case of quantitative analysis of XRF, it suggested that seven potassium atoms were detected for each **1**$_{CdNa}$ molecule. If we combine both results, the position of the potassium atom could be clearly identified at the linker site, whereas the other potassium site could not be resolved by X-ray diffraction due to severe disorder surrounding the cage structure.

In addition to that, the crystal structure of **5** showed prominent structural transformation than **2** and **3**. After soaking **1**$_{CdNa}$ in $CsNO_3$ solution, Cs^{I} ion was not occupied the position of Na^{I} but it became a new additional Cs^{I} linker atom positioned near Na^{I} (Fig. 1). The incorporation of Cs^{I} in **5** was confirmed by SCXRD, ^{133}Cs-NMR (δ = 6.70 ppm), and XRF analysis (Figs. 1-2). Previously, intermolecular interaction of two cage molecules in **1**$_{CdNa}$ initiated through π-π interaction between two benzene rings. In **5**, the new linker inserted between these aromatic rings forms a stabilizing interaction through the Cs^{I}, resembling the sandwich-type arrangement benzene-Cs^{I}-benzene (Fig. 2, see Ref. 11). The present of the additional Cs^{I} in the **5** expanded the lattice parameters and crystal volume, as expected from its ionic size. Oppositely, the SCSC reaction of **1**$_{CdNa}$ in Sr^{II} solution, structure refinement revealed no

transmetallation within the cage framework. Instead, Sr was detected outside the cage structure and existed as a metal-hydrate form (Table 1; Fig. 1). The presence of Sr in **5** was further confirmed by XRF analysis.

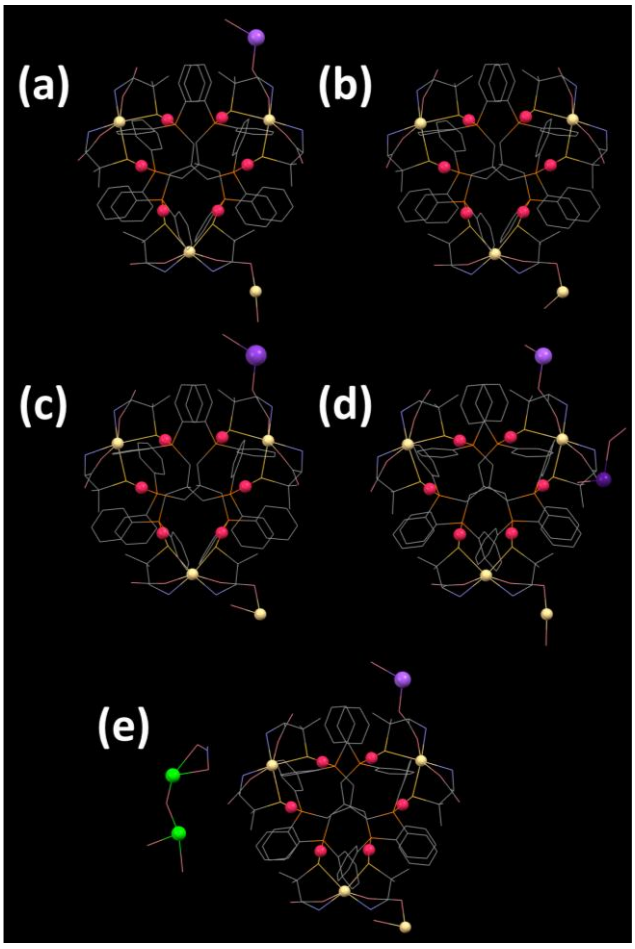

Figure 1. A perspective view of the asymmetric unit of (a) $\mathbf{1}_{\mathbf{CdNa}}$, (b) **2**, (c) **3**, (d) **4**, and (e) **5**. Color codes: red, Au; Cd, cream; Na; light purple, K; purple, Cs; pale purple, Sr; green, P; yellow, S; pink, O; pale blue, N; grey, C. The H atoms are omitted for clarity.

Here, we propose that replacement of the Cd^{II} metal center is inherently difficult because monovalent alkali metals and divalent alkaline-earth metals lack accessible *d*-orbitals to accept electron density from the coordinating organic ligands. Increasing the concentration of the metal-ion solutions from 1 M to 3 M did not promote metal exchange at this site, further supporting the resistance of the Cd^{II} center toward substitution. In the case of Sr^{II}, its high hydration energy and strong preference for forming highly coordinated aqua complexes made transmetallation even less favorable. As a result, Sr^{II} preferentially formed a hydrated species outside the cage rather than participating in metal exchange within the framework.

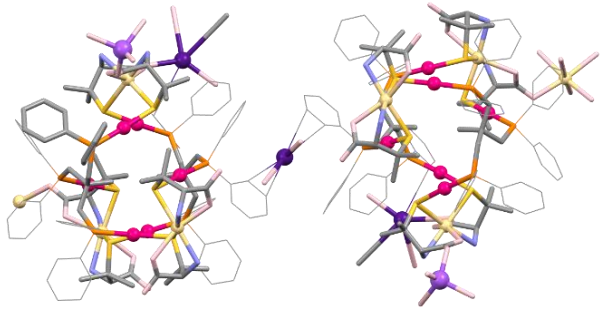

Figure 2. A perspective view of **4**. The position Cs^{I} additional linker between two benzene rings from different cage molecules. Color codes: red, Au; Cd, cream; Na; purple, Cs; pale purple, P; yellow, S; pink, O; pale blue, N; grey, C. The H atoms are omitted for clarity.

4. Conclusion

The transmetallation reactions of alkali and alkaline-earth metal ions in $\mathbf{1}_{\mathbf{CdNa}}$ were successfully investigated using single-crystal X-ray crystallography. Under the SCSC conditions, metal exchange occurred exclusively at the metal-linker position, where weak metal–oxygen interactions connect two cage molecules to form the supramolecular framework. In contrast, none of the metal-ion candidates were able to access or replace the six coordinate Cd^{II} centers bound to two D-penicillamine ligands. This resistance arises from the absence of *d*-orbitals in alkali and alkaline-earth metal ions, as well as their fundamentally different coordination preferences, which make substitution at the Cd^{II} metal center site energetically unfavorable.

Author contributions

Methodology: Benny Wahyudianto and Tatsuhiro Kojima. **Validation:** Tatsuhiro Kojima and Nobuto Yoshinari. **Formal analysis and writing—original draft preparation:** Benny Wahyudianto. Single-crystal X-ray measurement: Benny Wahyudianto, Tatsuhiro Kojima. **Writing—review and editing:** Benny Wahyudianto **Supervision:** Benny Wahyudianto, Nobuto Yoshinari, and Takumi Konno. All authors have read and agreed to the published version of the manuscript.

Conflicts of interest

There are no conflicts to declare.

Acknowledgement

The corresponding author (B.W.) is currently working at the National Institute of Advance Industrial Science and Technology (AIST) in Tsukuba, Japan.

References

[1] S. B. Khan, S-L. Lee, Supramolecular Chemistry: Host–Guest Molecular Complexes, *Molecules* **26**, 13 (2021) 3995. https://doi.org/10.3390/molecules26133995

[2] Y. Peng, H. Huang, Y. Zhang, C. Kang, S. Chen, L. Song, D. Liu, C. Zhong, A versatile MOF-based trap for heavy metal ion capture and dispersion, *Nat Commun* **9** (2018) 187. https://doi.org/10.1038/s41467-017-02600-2

[3] D. A. Rothschild, Z. Cao, F. Xie, B. Thomas, T. J. Emge, J. Li, T. Asefa, M. C. Lipke, Using Host-Guest Chemistry to Examine the Effects of Porosity and Catalyst-Support Interactions on CO_2 Reduction, *Angew. Chem.* **137**, 21 (2025) e202504630. https://doi.org/10.1002/ange.202504630

[4] T. Kawamichi, T. Haneda, M. Kawano, M. Fujita, X-ray observation of a transient hemiaminal trapped in a porous network, *Nature* **461** (2009) 633–635. https://doi.org/10.1038/nature08326

[5] B. Wahyudianto, T. Kojima, N. Yoshinari, T. Konno, The X-Ray Crystallography Evidence of Selective Co-Crystallization Between $[Au^{I}_{6}Ag^{I}_{3}Cu^{II}_{3}]^{3+}$ Chiral Metallo-Supramolecular Complex and Λ-$[Co(EDTA)]^{-}$ Isomer, *Indones. J. Chem.* **25**, 6 (2025) 1954–1962. https://doi.org/10.22146/ijc.105741

[6] B. Wahyudianto, T. Kojima, N. Yoshinari, T. Konno, Selective co-crystallization of $[Au^{I}_{6}Ag^{I}_{3}Cu^{II}_{3}]^{3+}$ and $[M^{I}_{3}Co^{III}_{2}]^{3-}$ (M = Au/Ag) complexes containing penicillamine ligand, *Polyhedron* **283** (2016) 117821. https://doi.org/10.1016/j.poly.2025.117821

[7] Y. Li, J. Yu, Emerging applications of zeolites in catalysis, separation and host–guest assembly, *Nat. Rev. Mater* **6** (2021) 1156–1174. https://doi.org/10.1038/s41578-021-00347-3

[8] J. Wang, W. Lin, V. O. Nikolaeva, R. Javaid, N. M. Khashab, Designing supramolecular pastes by controlling host–guest dynamics in reconfigurable networks, *Nat. Commun* **16** (2025) 7618. https://doi.org/10.1038/s41467-025-63033-w

[9] K. S. Walton, R. Q. Snurr, Applicability of the BET Method for Determining Surface Areas of Microporous Metal−Organic Frameworks, *J. Am. Chem. Soc.* **129**, 27 (2007) 8552–8556. https://doi.org/10.1021/ja071174k

[10] M. A. Muttaqii, D. C. Birawidha, K. Isnugroho, M. Amin, Y. Hendronursito, A. D. Istiqomah, D. P. Dewangga, The Effect of Chemical Activation by using Acid and Base Solution on Natural Zeolite Characteristics, *Jurnal Riset Teknologi Industri* **13**, 2 (2019) 266-271. DOI:10.26578/jrti.v13i2.5577

[11] K. Imanishi, B. Wahyudianto, T. Kojima, N. Yoshinari, T. Konno, A 116-nuclear metallosupramolecular cage-of-cage showing multistep single-crystal-to-single-crystal transformation, *Chem. Eur. J.* **26** (2020) 1827–1833. https://doi.org/10.1002/chem.201904275

[12] H. Takeda, T. Kojima, N. Yoshinari, T. Konno, A mesoporous ionic solid with 272 $Au^{I}_{6}Ag^{I}_{3}Cu^{II}_{3}$ complex cations in a super huge crystal lattice, *Chem. Sci.* **12** (2021) 11045–11055. https://doi.org/10.1039/D1SC02497C

[13] V.F. Yusuf, N. Malek I, S.K. Kailasa, Review on metal–organic framework classification, synthetic approaches, and influencing factors: applications in energy, drug delivery, and wastewater treatment, *ACS Omega* 7, 49 (2022) 44507–44531. https://doi.org/10.1021/acsomega.2c05310

[14] J. Guo, X. Xue, H. Yu, Y. Duan, F. Li, Y. Lian, Y. Liu, M. Zhao, Metal-organic frameworks based on infinite secondary building units: recent progress and future outlooks, *J. Mater. Chem. A* **10** (2022) 19320–19347. https://doi.org/10.1039/D2TA03159K

[15] K. Imanishi, B. Wahyudianto, T. Kojima, N. Yoshinari, T. Konno, A 116-nuclear metallosupramolecular cage-of-cage showing multistep single-crystal-to-single-crystal transformation, *Chem. Eur. J.* **26** (2020) 1827–1833. https://doi.org/10.1002/chem.201904275

[16] S. Surinwong, N. Kuwamura, T. Kojima, N. Yoshinari, A. Rujiwatra, T. Konno, Highly porous ionic solids consisting of $Au^{I}_{3}Co^{III}_{2}$ complex anions and aqua metal cations, *Inorg. Chem.* **60**, 16 (2021) 12555–12564. https://doi.org/10.1021/acs.inorgchem.1c01877

[17] N. Yoshinari, N. Kuwamura, T. Kojima, T. Konno, Development of Coordination Chemistry with Thiol-containing Amino Acids, *Coord. Chem. Rev.* **474** (2023) 214857. https://doi.org/10.1016/j.ccr.2022.21485

[18] N. Yoshinari, T. Konno, Multitopic metal-organic carboxylates available as supramolecular building units, *Coord. Chem. Rev.* **474** (2023) 214850. https://doi.org/10.1016/j.ccr.2022.214850

[19] B. Wahyudianto, K. Imanishi, T. Kojima, N. Yoshinari, T. Konno, Intermediate snapshots of a 116-nuclear metallosupramolecular cage-of-cage in a homogeneous single-crystal-to-single-crystal transformation, *Chem. Commun.* **57** (2021) 6090–6093. https://doi.org/10.1039/D1CC02219A

[20] Y. Inokuma, M. Kawano, M. Fujita, Crystalline molecular flasks, *Nat. Chem* **3** (2011) 349–358. https://doi.org/10.1038/nchem.1031